Rayleigh-Taylor instability of a particle packed viscous fluid: Implications for a solidifying magma

Hiroki Michioka and Ikuro Sumita

Department of Earth Sciences, Faculty of Science, Kanazawa University, Kanazawa, Japan

Received 24 October 2004; revised 10 January 2005; accepted 19 January 2005; published 11 February 2005.

[1] We performed laboratory experiments of Rayleigh-Taylor instability of superposed viscous fluids where the upper layer contains denser spherical solid particles. A series of experiments are made by varying the viscosity and the particle diameter, and we measure the growth rate and the wave length of the instability. The instability consists of fine-scaled plumes, which coalesce as they descend. Plumes are observed to form intermittently and the particle layer thins with time, which finally descend as blobs. We find that the growth rate can be explained by using the linear stability analysis for Rayleigh-Taylor instability of viscous fluids, by taking the effective viscosity of particle bed to be 20 times that of the fluid, and scale the thickness of the upper layer by twice the particle diameter. Using this scaling, we find that a partially solidified layer beneath the surface of a lava lake may become unstable by this mechanism. **Citation:** Michioka, H., and I. Sumita (2005), Rayleigh-Taylor instability of a particle packed viscous fluid: Implications for a solidifying magma, *Geophys. Res. Lett.*, *32*, L03309, doi:10.1029/2004GL021827.

1. Introduction

[2] Rayleigh-Taylor (R-T) instability is ubiquitous in nature. For superposed layers of two Newtonian viscous fluids, the growth rate and the wave length of instability are well studied [e.g., *Chandrasekhar*, 1961]. An example of such instability is possible in a solidifying lava lake, where the heavier crystal bearing magma at the surface of the lake may become unstable and sink. It may also occur in a magma chamber, where the mushy layer develops from the roof. It has been proposed that such instability may be responsible for the formation of silicic segregations [*Marsh*, 2002].

[3] The presence of crystals in magma not only increases the viscosity, but also causes the fluid to possess finite yield strength and shear thinning viscosity [e.g., *Lejeune and Richet*, 1995] and may behave similar to a granular flow. Laboratory experiments have been used to study R-T instability of such fluids containing particles. *Thomas et al.* [1993] found that the instability take the form of plumes. *Voltz et al.* [2000, 2001] studied a similar case in a Hele-shaw like geometry and measured the growth rate and the wave length of the instabilities for both a high packing fraction case $\phi = 0.61$ [*Voltz et al.*, 2000], and a low packing case $\phi < 0.065$ [*Voltz et al.*, 2001]. However in these studies, no detailed results were given regarding the parameter (i.e., viscosity and particle size) dependences, which are relevant if we wish to scale to geological situations. Here, we report the results of a series of experiments for a highly packed case, focusing on how the growth rate and wave length depends on viscosity and particle size spanning by 4 orders and 1 order of magnitude, respectively.

0094-8276/05/2004GL021827$05.00

2. Experimental Methods

[4] Our experimental cell is a plastic styrol container of 35 mm height, 65 mm length and 10 mm width which allows the flow to become 3-D. The width is thicker by 5 times compared to that used by *Voltz et al.* [2000, 2001]. To examine the effect of the cell size, we also perform experiments using a larger cell with a dimension of 194 $\times$ 102 $\times$ 26 mm. Two types of viscous fluids are used. One type is glycerine solution. It was used in concentrations of 62, 81 and 99 wt% with a viscosity range of $4.21 \times 10^{-3} < \eta < 7.75 \times 10^{-1}$ Pas. The other is a silicone oil with different batches spanning a viscosity range of $9.65 \times 10^{-2} < \eta < 9.75$ Pas. For experiments using glycerine solution, we placed the cell in an isothermal bath with temperatures of 25°C and 50°C controlled at a precision of <0.1°C. For solid particles, we used soda-lime glass beads (Toshin Ricoh) with 8 different mean particle diameters in the range of 50 μm $\leq d \leq$ 850 μm. We measured the particle diameter by a microscope and confirmed the values provided by the manufacturer. Resulting Reynolds number based on initial wave length and growth rate is small; $Re \leq 0.1$.

[5] The experimental procedure is as follows. First, the cell was inverted and the layer of glass beads was allowed to completely settle and compact for 4–5 days. The packing fraction of the glass beads layer was calculated to be approximately $\phi = 0.6$ from the weight and height of the layer. This value is close to that of a dense random packing $\sim$0.64 [*Mavko et al.*, 1998]. This procedure was repeated once more and then the experimental run was made. The images were recorded using a digital video camera. The growth rate of the instability was measured by tracking the tip of the fastest growing plume. The average spacing of the plumes was obtained from the side image.

3. Results

3.1. Evolution of the Instability

[6] Figure 1 shows a typical time evolution of the instability for a fluid viscosity of 9.75 Pas and a particle diameter of 115 μm. The initial instability consists of very fine-scaled plumes with an average lateral spacing of 1.8 mm. The lateral movement within the compacted layer at this stage is confined to the lowermost part of the layer with a thickness of several grain sizes. With the growth of

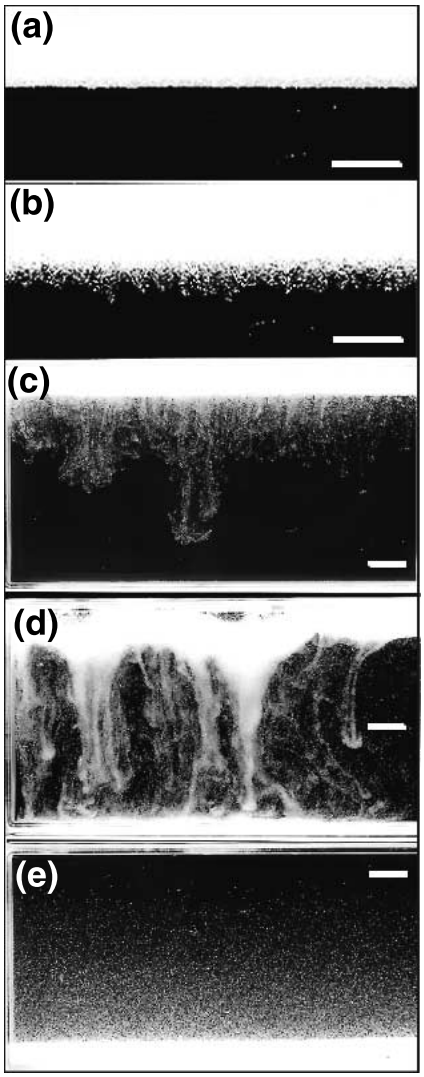

Figure 1. Time-evolution of the instability of a silicone oil and glass beads mixture with an initial packing fraction of 0.6. Fluid viscosity is $\eta = 9.75$ Pas and the particle diameter is 115 μm. The scale bar is 5 mm. (a) $t = 0$ (s), (b) $t = 1140$ (s), fine-scaled instability with an average wave length of 1.8 mm, (c) $t = 2190$ (s), a developed instability from plume coalescence and mixing, (d) $t = 3810$ (s), instability with a longer wave length and formation of an arch-like interface, (e) $t = 19140$ (s), final stage of hindered settling. Reynolds number based on typical length and velocity scale is $\leq 10^{-4}$ for all stages.

the instability, adjacent plumes coalesce as they descend downwards, and form distinct plume heads. The plume is unsteady, and is observed to form intermittently in a manner similar to boundary layer instability of thermal plumes. As the top layer becomes thinner, compacted blobs of glass beads peel off from the upper boundary. In the final stage, particles of glass beads slowly settle and a clear fluid layer emerges from the top whose front descends downward (i.e., hindered settling). A layer of glass beads at the base slowly compacts until the thickness approach the initial value. For the case shown in Figure 1, the particle settling takes about 17.5 hours, after which further compaction occurs.

[7] The evolution of the location of the tip of the plume is shown in Figure 2. The instability initially increases exponentially with time, and then deviates from the exponential growth and approach a terminal velocity. We fit the height as a function of time as $h = h_0 \exp(\sigma t)$ by a least squares method. For h_0, the initial amplitude of instability, we take the particle diameter. We select the time range which minimizes the least squares error, and obtain the growth rate σ. The corresponding h used for the exponential fit is $h = 2.8 \pm 0.1$ mm and is uncorrelated with the viscosity value. Similarly, we obtain the terminal velocity from the linear fit. Up to 4–5 runs were made for the same viscosity, and we calculate the average value and their standard deviation. Experiments with larger cell size did not yield systematic difference in the growth rate. By varying the thickness of the upper layer, we found that for a thickness of 10 mm and larger, a long wave length instability occurs, where the central part sags downwards. This instability occurs simultaneously with the fine-scaled instabilities described above. In this paper, we analyze the results for a thickness of 5 mm where the long wave length instability does not occur.

3.2. Viscosity Dependence

[8] We made a series of experiments by varying the fluid viscosity by 4 orders of magnitude for a fixed particle size of 50 μm. Here, we define the wave length of instability by the average spacing between the plumes. From the experiments, we find that (1) the initial growth rate is approximately inversely proportional to the fluid viscosity (Figure 3), and (2) the initial wave length, $\lambda = 1$ mm, is independent of fluid viscosity. We note that in Figure 3, the variation of density difference between the fluid used and the glass beads is small for different viscosities. It is <2.8% for glycerine solution and <0.34% for silicone oil. We also remark that the data points for glycerine solution and silicone oil overlap in the viscosity range of 0.1 to 1 Pas. The overlap for two different fluids used indicates that the difference of interfacial tension between the glass beads and the fluids has a negligible effect on the growth rate.

3.3. Particle Size Dependence

[9] We next made a series of experiments by varying the particle size by an order of magnitude for two cases of fixed

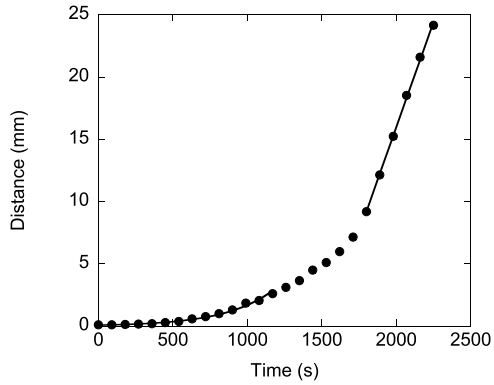

Figure 2. An example of the growth of the instability by tracking the tip of the plume head ($\eta = 9.75$ Pas, particle size 115 μm). The initial exponential fit and later linear fit for terminal velocity is shown.

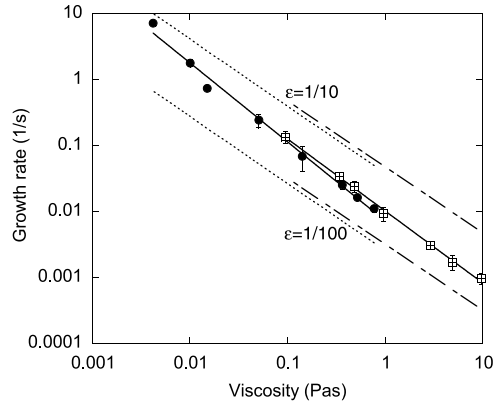

Figure 3. Viscosity dependence of the growth rate for a particle diameter of 50 μm. Circles and squares are data for glycerine solution and silicone oil, respectively. Solid lines are power law fit of the data with exponents of −1.20 for glycerine solution and −1.09 for silicone oil. 2 sets of dotted and broken lines are theoretical growth rates for glycerine solution and silicone oil, respectively, for 2 values of viscosity contrast (ϵ) shown.

viscosity. The thickness of the particle layer was kept fixed at 5 mm. Experiments show that plumes can be identified for all particle size, but when the size exceeds 0.4 mm, the plume head consists of smaller number of particles and some particles were observed to fall discretely. From the experiments, we find that (1) the initial growth rate has a power law dependence against the particle size with an exponent of about 0.83 (Figure 4a), and (2) the average wave length of the initial instability λ (mm) has a similar power law dependence against particle diameter d (mm) for two different viscosities; $\lambda = 8.6 \times d^{0.79}$ for $\eta = 2.91$ Pas and $\lambda = 12.0 \times d^{0.88}$ for $\eta = 9.75$ Pas (Figure 4b).

4. Scaling Analysis

[10] We analyze our results by applying the linear stability analysis of R-T instability of two Newtonian viscous fluids by *Whitehead and Luther* [1975]. When the viscosity of the thin layer is very large, the wavelength of the instability is given by

$$\lambda = \frac{4\pi h}{(180\epsilon)^{1/5}} \tag{1}$$

and the growth rate by

$$\sigma = \frac{\Delta\rho g h}{4\mu_2}\epsilon\left(1 - 0.443\epsilon^{4/5}\right) \tag{2}$$

where

$$\epsilon = \frac{\mu_2}{\mu_1} \tag{3}$$

is the viscosity ratio of the thin upper(1) to the thick lower(2) layer. Here h is the thickness of the thin layer and $\Delta\rho$ is the density difference between the two fluids.

[11] We apply this model to our experiments. First we consider the results shown in Figure 3. From $\lambda = 1$ mm, we substitute equation (1) into equation (2), and calculate σ for glycerine solution and silicone oil, with ϵ as the parameter. Here, we calculated the σ for a same set of η and $\Delta\rho$ as in the experiments. The lines connecting these points are shown in Figure 3 and we find that $\epsilon \simeq 1/20$ best explains the experiments, which imply that the layer of glass beads behaves as a viscous fluid with an effective viscosity of 20 times that of the fluid layer. From equation (1), we obtain $h \simeq 0.1$ mm, which shows that the effective thickness is about twice the particle diameter. This thickness is also consistent with our observation that only the bottom most layer of the glass beads is mobile. We can compare this result with the formula for the effective viscosity of a fluid containing solid particles. A commonly used Einstein-Roscoe equation [*McBirney and Murase*, 1984] gives,

$$\epsilon = (1 - \phi/\phi_{\max})^{2.5} \tag{4}$$

where ϵ is the ratio of viscosity of the liquid to the viscosity of liquid containing solid particles, $\phi_{\max}$ is the maximum packing fraction. We take $\phi_{\max} = 0.6$, and for $\epsilon = 1/20$ which best explains our experiments shown in Figure 3, we obtain $\phi = 0.42$. This result implies that the packing fraction in the plumes is reduced from the initial value and that the particles in the plumes have moved away from each other which is consistent with the video images. We have also analyzed the terminal velocity and find that the velocity scales as $\propto\mu^{-1}$, which is consistent with Stokes flow with plume head size independent of viscosity.

[12] We next consider results shown in Figure 4. Using the empirical relationship between λ and d, we similarly calculate the theoretical growth rate as shown in Figure 4 with ϵ as the parameter. We find that $\epsilon \simeq 1/17$ best explains the experimental result and that effective layer thickness h is about twice the particle size. These results are consistent with the results obtained by varying the viscosity. The increase of the wave length of the instability with particle size can be interpreted as a consequence of the increase of the effective layer thickness h with particle size.

5. Discussion

[13] In our experimental parameter range, we found that the initial growth rate can be explained by linear stability

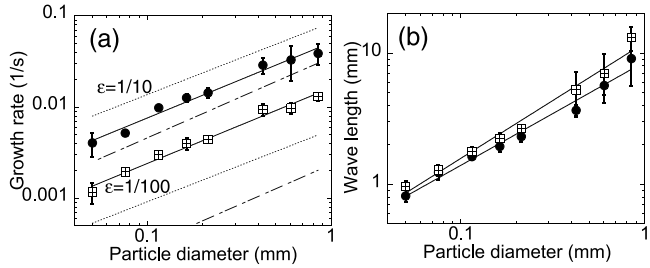

Figure 4. (a) Particle diameter dependence of the growth rate for silicone oil of $\eta = 2.91$ Pas (circles) and $\eta = 9.75$ Pas (squares). Solid lines are power law fit of the data both with exponents of 0.83. 2 sets of dotted and broken lines are theoretical growth rates for viscosity of $\eta = 2.91$ Pas and $\eta = 9.75$ Pas respectively, for 2 values of viscosity contrast (ϵ) shown. (b) Particle diameter dependence of the wave length of the initial instability with power law fits. Marks correspond to cases shown in (a).

theory for viscous fluids by introducing the effective values for viscosity and layer thickness implying that we can approximate the layer of solid particles as a continuum medium. The thin effective thickness of about 2 particle size indicate that most of the particle packed viscous fluid is initially immobile. A possible reason for this is that the shear stress resulting from the instability is less than the yield strength except near the interface with the liquid layer. The application of the linear stability theory is validated by small Reynolds number at initial stage of the instability. However at later stages, experiments with small viscosity yield $Re > 1$. For the experiments shown in Figure 3, using the size and velocity of descending blobs, we find that $Re > 1$ for viscosity $< 5 \times 10^{-2}$ Pas.

[14] There are several situations where R-T instability of a crystal bearing magma may become important. One is in a lava lake which is solidifying from the surface. Another is a magma ocean where solidification proceeds from the base due to the pressure effect on the liquidus. Plagioclase crystals can become lighter than melt, and may float from R-T instability, and has been proposed as the mechanism for the formation of lunar highlands [e.g., *Anderson*, 1989]. For R-T instability to occur, the thinning rate of the mushy layer by the instability must be faster than the crystal capture by the progression of the solidification front. A lower limit for the thinning rate of the mushy layer can be evaluated using our experimental results. We consider a basaltic magma with a density difference between the melt and crystal mush (crystallinity 0.6) of $\Delta\rho = 220$ kg/m^3. An order of magnitude estimate of thinning rate of the mush by the initial instability is given by $v = \frac{dh}{dt} \sim h_0\sigma \sim 10^{-7} \left(\frac{h_0}{0.1\,\mathrm{mm}}\right)\left(\frac{10\,\mathrm{Pas}}{\mu}\right)$(m/s). Here the typical crystal size is used for the estimate of h. Note that this estimate gives the lower limit since the actual thinning rate of the crystal layer become faster with time (Figure 2) and also as the particle layer loosens and become increasingly mobile. Our experiments show that the time-averaged thinning rate is 10 times faster than the above estimate. On the other hand, measured rate of the progression of the solidification front of a lava lake such as Makaopuhi in Hawaii is of the order of 10^{-7} m/s [*Wright et al.*, 1976] and the rate of the progression of the mush-liquid interface is estimated to be comparable [*Worster et al.*, 1993]. Although the actual crystals are aspherical and the rheology is even more complex, a comparison of the above two estimates shows that thinning of the crystal mush by R-T instability can become comparable to the measured progression of the solidification front, suggesting that this is an efficient mechanism of recycling crystals back to the molten magma. It also provides a mechanism to weaken the crystal mush layer which can eventually lead to subduction of rigid layer as observed in our experiments. The plate tectonics observed in lava lakes [*Duffield*, 1972] may have been initiated by such instability.

[15] **Acknowledgments.** We thank A. Namiki for discussions, M. Manga and an anonymous referee for review. This work was supported by Grant-in-aid for scientific research, Japan Society for the Promotion of Science.

References

Anderson, D. L. (1989), *Theory of the Earth*, 366 pp., Blackwell, Malden, Mass.

Chandrasekhar, S. (1961), *Hydrodynamic and Hydromagnetic Stability*, 652 pp., Dover, Mineola, N. Y.

Duffield, W. A. (1972), A Naturally occurring model of global plate tectonics, *J. Geophys. Res.*, *77*, 2543–2555.

Lejeune, A.-M., and P. Richet (1995), Rheology of crystal-bearing silicate melts: An experimental study at high viscosities, *J. Geophys. Res.*, *100*, 4215–4229.

Marsh, B. D. (2002), On bimodal differentiation by solidification front instability in basaltic magmas, part 1: Basic mechanics, *Geochim. Cosmochim. Acta*, *12*, 2211–2229.

Mavko, G., T. Mukerji, and J. Dvorkin (1998), *The Rock Physics Handbook*, 329 pp., Cambridge Univ. Press, New York.

McBirney, A. R., and T. Murase (1984), Rheological properties of magmas, *Annu. Rev. Earth Planet. Sci.*, *12*, 337–357.

Thomas, N., S. Tait, and T. Koyaguchi (1993), Mixing of stratified liquids by motion of gas bubbles: Application to magma mixing, *Earth Planet. Sci. Lett.*, *115*, 161–175.

Voltz, C., M. Schroter, G. Iori, A. Betat, A. Lange, A. Engel, and I. Rehberg (2000), Finger-like patterns in sedimenting water-sand suspensions, *Phys. Rep.*, *337*, 117–138.

Voltz, C., W. Pesch, and I. Rehberg (2001), Rayleigh-Taylor instability in a sedimenting suspension, *Phys. Rev. E*, *65*, doi:10.1103/PhysRevE.65.011404.

Whitehead, J. A., and D. S. Luther (1975), Dynamics of laboratory diapir and plume models, *J. Geophys. Res.*, *80*, 705–717.

Worster, M. G., H. E. Huppert, and R. S. J. Sparks (1993), The crystallization of lava lakes, *J. Geophys. Res.*, *98*, 15,891–15,901.

Wright, T. L., D. L. Peck, and H. R. Shaw (1976), Kilauea lava lakes: Natural laboratories for study of cooling, crystallization, and differentiation of basaltic magma, in *The Geophysics of the Pacific Ocean Basin and Its Margin: A Volume in Honor of George P. Woollard*, *Geophys. Monogr. Ser.*, vol. 19, edited by G. H. Sutton, M. H. Manghnani, and R. Moberly, pp. 375–390, AGU, Washington, D. C.

H. Michioka and I. Sumita, Department of Earth Science, Faculty of Science, Kanazawa University, Kanazawa, 920-1192, Japan. (sumita@earth.s.kanazawa-u.ac.jp)